Finding the sweet spot: a library of hydrogels with tunable degradation for tissue model development

Narendra Pandala[1], Michael A. LaScola[1], Zachary Hinton[2,3], LaShanda T.J. Korley[2,3], Erin Lavik[1]

[1]Department of Chemical, Biochemical and Environmental Engineering, University of Maryland Baltimore County, Baltimore, MD, Piscataway Territories, USA.

[2]Department of Materials Science and Engineering, University of Delaware, Newark, Delaware 19716, United States

[3]Department of Chemical and Biomolecular Engineering, University of Delaware, Newark, Delaware 19716, United States

Keywords: polyallylamine, poly-L-Lysine, facile synthesis, non-degradable gels, synthetic gels, kinetics, hydrogels, PAA, PAH, PAAm, and PA

ABSTRACT

In vitro models are valuable tools for applications including understanding cellular mechanisms and drug screening. Hydrogel biomaterials facilitate in vitro models by mimicking the extracellular matrix and in vivo microenvironment. However, it can be challenging for cells to form tissues in hydrogels that do not degrade. In contrast, if hydrogels degrade too much or too quickly, tissue models may be difficult to assess in a high throughput manner. In this paper, we present a poly(allylamine) (PAA) based synthetic hydrogel system which can be tuned to control the mechanical and chemical cues provided by the hydrogel scaffold. PAA is a polycation with several biomedical applications, including the delivery of small molecules, nucleic acids, and proteins. Based on PAA and poly(ethylene glycol) (PEG), we developed a synthetic non-degradable system with potential applications for long-term cultures. We then created a second set of gels that combined PAA with poly-L-lysine (PLL) to generate a library of semi-degradable gels with unique degradation kinetics. In this work, we present the hydrogel systems' synthesis, characterization, and degradation profiles along with cellular data demonstrating that a subset of gels supports the formation of endothelial cell cord-like structures.

INTRODUCTION

Hydrogels are water-soluble polymers crosslinked to form networks with applications for in vitro models, drug delivery systems, and tissue engineering[1-5]. Because of their mechanical properties that mimic tissue-like properties and ability to supplement with adhesive motifs and extracellular matrix (ECM) molecules, hydrogels act as ideal scaffolding material to provide the required mechanical and biochemical cues for in vitro applications [1, 6]. Hydrogels based on native materials like collagen, gelatin, and Matrigel act as good scaffolding materials, but their batch-to-batch variability presents a challenge in obtaining consistent material properties[7-11]. On the other hand, a synthetic biocompatible hydrogel might eliminate the issue of variability, giving a more consistent scaffolding material with uniform mechanical and chemical cues.

Poly(ethylene glycol) (PEG) is a widely used material because of its biocompatibility and versatility to modify the end groups to accommodate various crosslinking reactions[6, 12-14]. It is used both to tune natural and synthetic gel systems and other biomaterials[13-15]. Previously we have used PEG and poly-L-lysine (PLL)-based synthetic gel systems for tissue modeling applications[16-18]. These gels are enzymatically degradable. We have designed the PEG-PLL gels to be incorporated as a bioink for the screen printing based bioprinting process we have developed[18, 19]. We utilized succinimide and free amine chemistry to facilitate the crosslinking between PEG-PAA within an operable time crucial for the screen printing process[20]. One of the challenges with these degradable gels is that they may not be ideal when used as a scaffolding material for long-term cultures because some cell types, such as endothelial cells, can break down the hydrogels in a matter of days [21]. To leverage the benefits of the PEG-PLL system, including the ability to adsorb proteins onto the hydrogel matrix, we sought to combine a non-degradable component, poly(allylamine) (PAA), with PLL. Since PAA has amines, the same crosslinking chemistry can be used to make a non-degradable gel system with a similar gelation time making it suitable as a bioink in the screen-printing process.

PAA is a polycationic polymer of allylamine, which has several biomedical applications, including drug delivery[22], protein, and nucleic acid delivery by forming complexes known as polyplexes [23]. It is also used as a component of transfection agents [24] and in the synthesis of microgels[25] and anti-microbial coatings [26]. PAA can be modified to promote mucoadhesion which is ideal for drug delivery systems and in vitro models [27]. The PAA and PLL contain primary amines that react with a PEG succinimidyl glutarate (SG) crosslinker based on the succinimidyl-amine conjugation reaction [20]. In this paper, we investigate a library of hydrogels based on blends of PLL and PAA with PEG-SG and determine the relationship between the mechanics, degradation, and cord formation of vascular cells in vitro. In this work, we have abbreviated polyallylamine as PAA following one of the acronyms used in the literature[28-30]. There have also been other naming conventions including PAH[31], PAAm[27], and PA[26] used for the same polymer.

RESULTS

Synthesis of precursors and hydrogel fabrication

The hydrogels are synthesized using PAA (120-200kDa) and PEG-SG (Figure 1A, Figure S1) based on the free amine and succinimidyl chemistry (Figure 1B). Initially, PEG is functionalized to form PEG-SG using the succinimidyl reaction[20]. Next, the formation of the PEG-SG is confirmed using the ^{1}H NMR (Figure S2). This synthesized PEG-SG is then used to react with

PAA (120-200kDa), which provides the amines to form a crosslinking network forming the hydrogel (Figure 1).

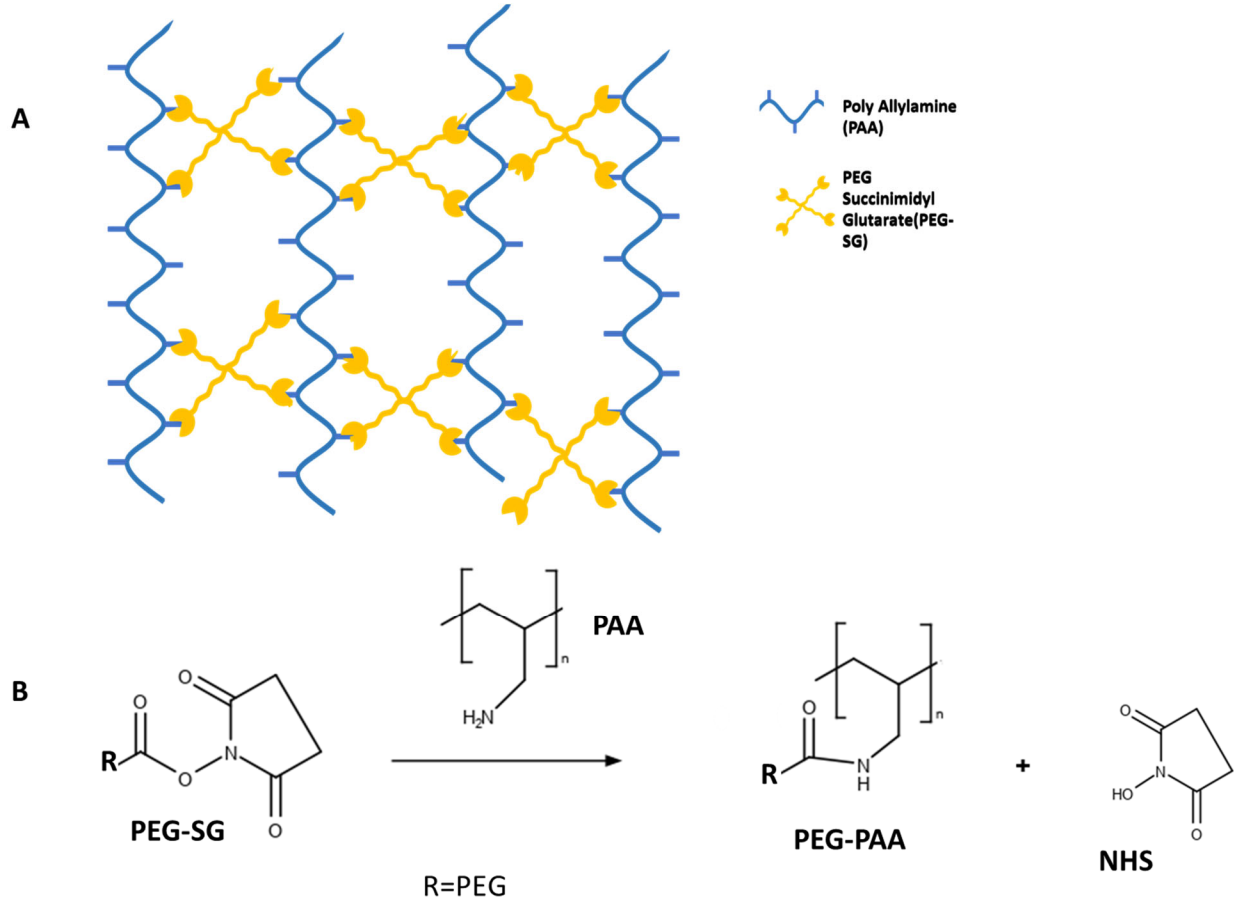

Figure 1. A) Schematic of the PEG-PAA hydrogel formation based on 4 arm PEG-SG and PAA, where the crosslinking occurs by the B) succinimidyl and free amine reaction.

PEG-PAA hydrogel properties

10% w/vol precursor solutions of PEG-SG and PAA in either PBS or culture media were combined to create a library of gels by altering the relative amounts of the two components to form the hydrogels. Initially, two sizes of PEG-SG (bifunctional 4.6kDa and 4-arm 10kDa) were tested to synthesize the hydrogel (the data corresponding to the 4arm PEG is presented in the main text, and some data corresponding to the 2-arm PEG is presented in the supplementary information). A library of hydrogels was synthesized by varying the ratios of free amines in PAA to succinimides in PEG (the hydrogel synthesized using the 1:1 ratio of the reactive groups resulted in a non-homogenous gel containing gel-like and liquid-like components, so that ratio was not used for analysis).

Small amplitude oscillatory shear (SAOS) measurements were performed to characterize the frequency-dependent storage moduli (G') of the hydrogel library (Figure 2A, Figure S3). As the free amine-succinimide ratio increases, the modulus steadily increases by an order of magnitude

from 2:1 to 6:1, after which a decrease is observed (Figure 2A,2B). This trend is consistent with changing the crosslink density with different PEG-SG content (i.e., modulus proportional to the degree of crosslinking)[32]. Furthermore, as the ratio of amines to SG groups increases beyond 10:1, a more pronounced decrease in G' is observed. This approach toward transitional behavior suggests the 50:1 gel (which has the lowest amount of crosslinker) is approaching the critical gelation concentration for this system[32]. Figure S4 shows the calculated molecular weight between crosslinks obtained from the storage modulus of the system[33, 34]. The non-monotonic dependence of G' on the amount of crosslinker (Figure S4) is typical behavior for many gels. Increasing crosslinker concentration does not contribute to elastically active network structures because of network inhomogeneity, including cyclization, single-site-bound crosslinkers, and nanogel clusters[35]. Scanning electron microscopy (SEM) was used to observe the network structure of the hydrogels (Figure 2C) and showed that there were macro and micropores through the material, something typically seen with PEG-polycationic gels [16, 17]. Both pore sizes from SEM micrographs and moduli illustrate the evolving microstructure determined by crosslink density. In conjunction with the pore size noticed in all the hydrogels, a larger pore structure was observed in the hydrogels with lower moduli (2:1, 20:1, and 50:1 ratios) (Figure S5).

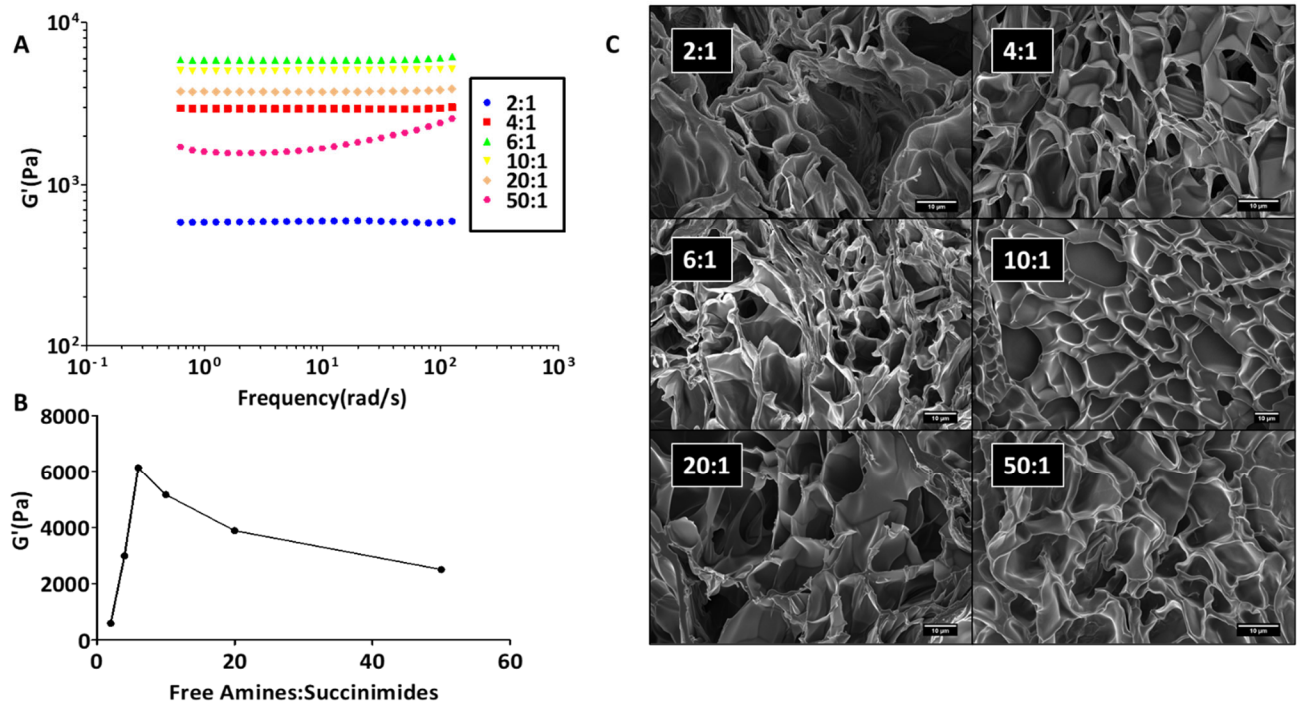

Figure 2: A) Frequency-dependent storage modulus (G') of PEG-PAA hydrogels with varied ratios of free amines to succinimidyl groups; B) Average storage modulus for the frequency-independent region of (A) as a function of the free amine ratio; C) SEM micrographs of the hydrogels (Scale bar is 10μm)

Cell survival on the PEG-PAA hydrogels

To test the biocompatibility of the hydrogels, rat endothelial cells (RECs) seeded on top of the hydrogels base were synthesized using the culture media without any supplementation from extracellular matrix proteins (ECM) or any adhesive agents (like PLL or collagen). It was

observed that all the ratios, except the 50:1 ratio, showed excellent short-term survival (Figure 3A, B). Similar trends were observed using a hydrogel system synthesized using bifunctional PEG and PAA supplemented with 1% laminin using the Caco-2 cells (Figure S6-S7). The facile synthesis of the precursors and the optical clarity of the gels (the gels are transparent with a yellowish hue) coupled with the tunability of the gel system all lead to a strong foundation for in vitro tissue models.

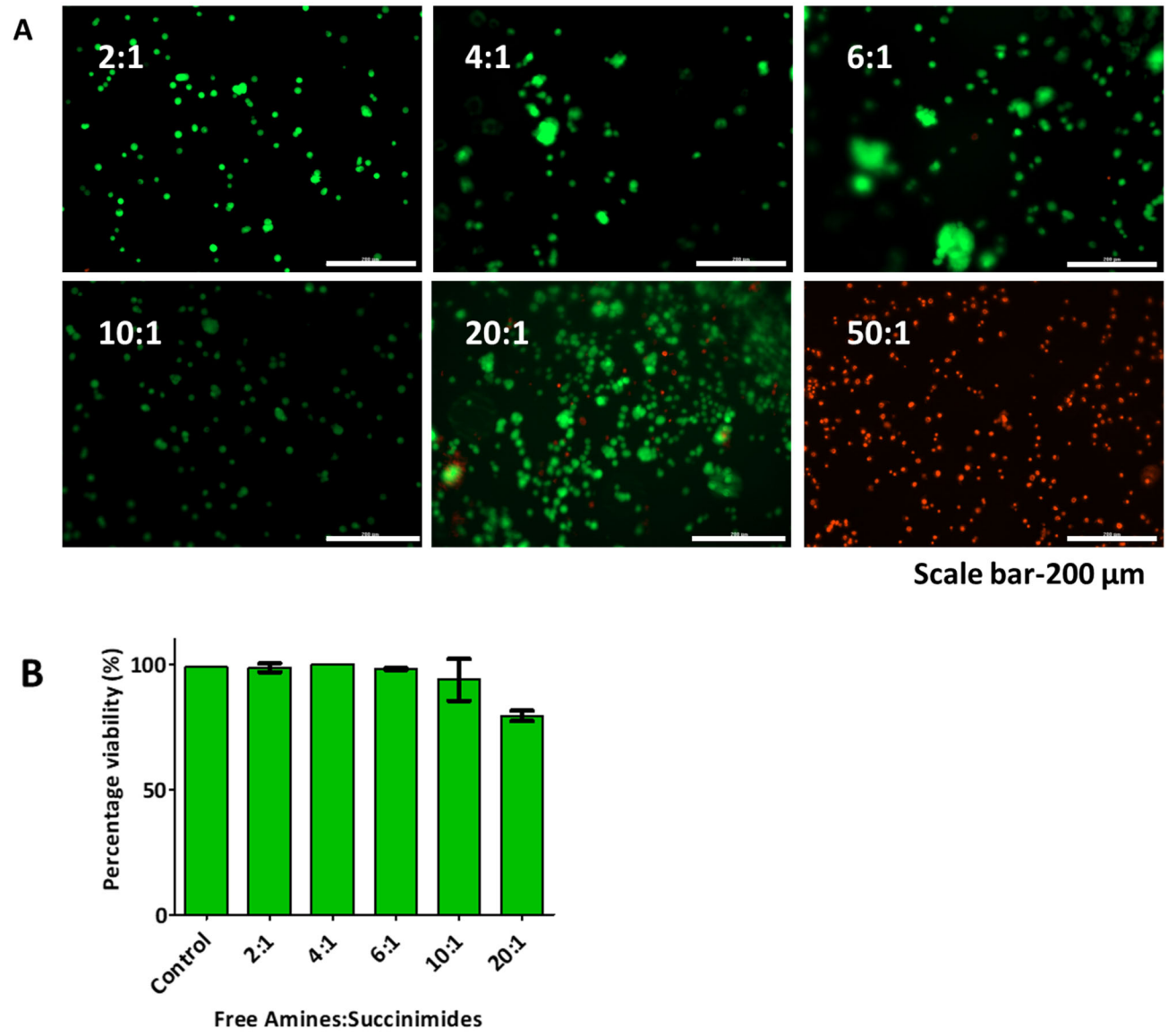

Figure 3. A) Images showing the live/ dead scans of rat endothelial cells seeded on top of the PEG-PAA hydrogel library, calcein-AM is used to stain the live cells, and ethidium homodimer-1 is used to stain dead cells (Scale bar is 200 µm). B) Quantification of the survival of the cells on various PEG-PAA hydrogels, (the 50:1 ratio was not included in the quantification since no live cells were found on that gel.)

Semi-degradable PEG-PAA-PLL hydrogel

The PEG-PAA gel system was not degradable either by hydrolysis or enzymatically by trypsin. Given that linear PLL has been shown to degrade in trypsin[36], we developed a PEG-PLL-based hydrogel system using similar chemistry[18]. We observed that PEG-PLL hydrogels degrade completely within 3 hours in trypsin. Utilizing the contrasting nature of both these systems, we create a semi-degradable hydrogel library using both the PAA and PLL crosslinked with PEG-SG. We used three mixtures of PAA and PLL (25%, 50%, and 75% PLL, where the percentage of PLL in the PAA-PLL mixture is calculated as a fraction of the free amines) to create the PEG-PAA-PLL library (Figure 4A, Figure S1).

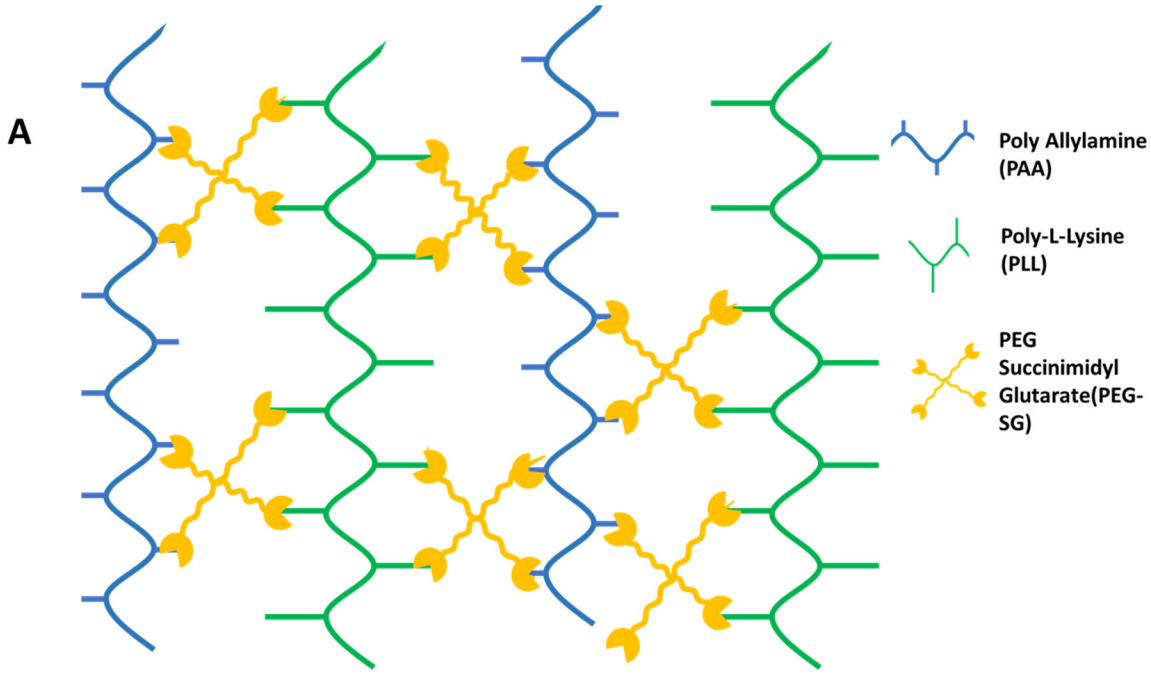

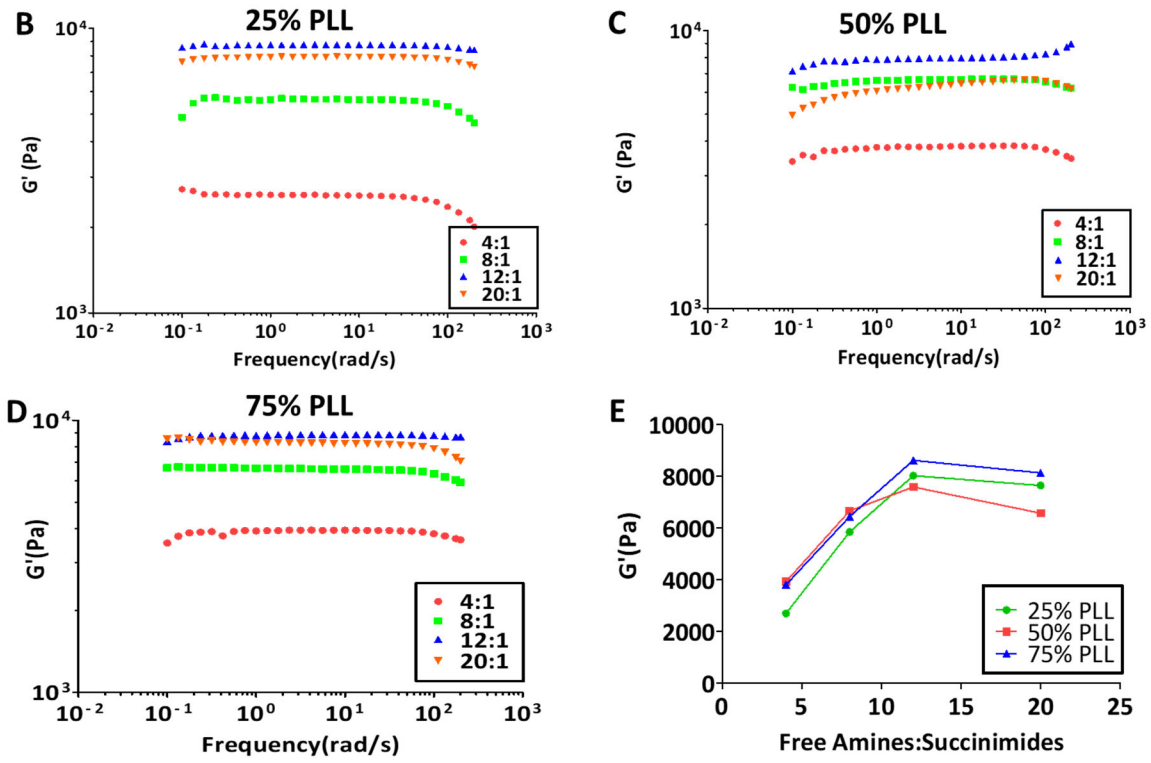

Figure 4.A) Schematic of the formation of the PEG-PAA-PLL hydrogels system utilizing the same succinimidyl amine reaction, replacing the some of the PAA in the system with enzymatically degradable PLL. B-D) Frequency dependence of the storage moduli of gels spanning different PLL content and free amine to succinimide ratio. E) Average storage moduli from the frequency-independent portions of (B-D) for each set of PLL concentrations as a function of the free amine ratio.

The storage moduli of this library were determined using SAOS (Figure 4B-D, Figure S8). The moduli for each series of gels at fixed PLL concentration follow the same trend for PEG-PAA gels. Many gels exhibit a reduction in modulus at high frequencies (> 100 rad/s). This has been seen with other hydrogel systems [34, 37, 38] and may be a function of a combination of the hydrogel behavior and experimental setup. For experimental simplicity, it is preferable to utilize pre-formed gels, which often undergo slip between the plate surfaces and the gel at high frequencies. Using in situ gelation of two different compositions, we confirmed that the measured storage moduli obtained using pre-formed gels and those gelled in the rheometer (where slip is unlikely) were similar (Figure S9). There was a noticeable difference between strain sweep behavior. In the case of pre-formed gels, an apparent critical strain is observed, after which the storage and loss moduli converge and eventually cross. Subsequent frequency sweeps led to identical behavior as the pre-strain sweep. Therefore, the apparent linear viscoelastic regime (where storage and loss moduli are independent of strain) represents the absence of slip, which occurs beyond the apparent critical strain amplitude. Because slip does not involve the bulk gel, no structural changes were observed. In the case of the in situ gelled samples, this was not the case. Instead, a higher (true) critical strain was observed, at which storage and loss moduli simultaneously converge and decrease (Figure S10). Subsequent frequency sweeps show an order of magnitude reduction in storage modulus, indicating that the observed viscoelastic

regime is accurate and that high strains damage the gel. In all cases, loss modulus was more challenging to measure due to its relatively low magnitude and variability. For this reason, we have only included these data in the supporting information for completeness (Figure S3, S8). Nevertheless, we can conclude that measurements of the storage moduli of pre-formed gels are valid given strains in the no-slip (apparent viscoelastic) window. However, quantification of gel-breakup phenomena cannot be adequately observed without good gel adhesion to the plates, ideally by formation in situ, or by a more specialized geometry.

From this analysis, similar trends to PEG-PAA gels are observed in the average storage moduli of the PEG-PAA-PLL gels; that is, modulus increases up to a critical free amine ratio after which decreased moduli are observed (Figure 4E). This behavior is likely a consequence of network defects resulting from increased crosslinker content and varied pore structure of the gels. It should be noted that G' are far less sensitive to PLL content than to crosslinker content (Figure 4E), meaning tunability of degradation can be achieved with little change to modulus.

Degradation kinetics of the PEG-PAA-PLL hydrogel

Since the combined gel system has both degradable and non-degradable components, we measured the enzymatic degradation profiles of this gel library by observing the difference in dry weight after being exposed to trypsin (Figure 5A-C). The data showed that the 25%, 50%, and 75% PLL gels on an average lost 10%, 17%, and 24% respectively of dry weight after trypsinization for 72 hours. Since the gels were structurally intact after 3 days with a reduction in weight, we modeled the degradation kinetics using pseudo-first-order kinetics with a residual weight fraction term to account for the final weight of the gel ($w/w_o=(1-R_w)exp(-k_Dt)+R_w$) (Figure 5A-D). The degradation rate constant(k_D), predicted residual weight fraction (R_w), and the coefficient of determination (R^2) of the model fits are shown in Table 1.

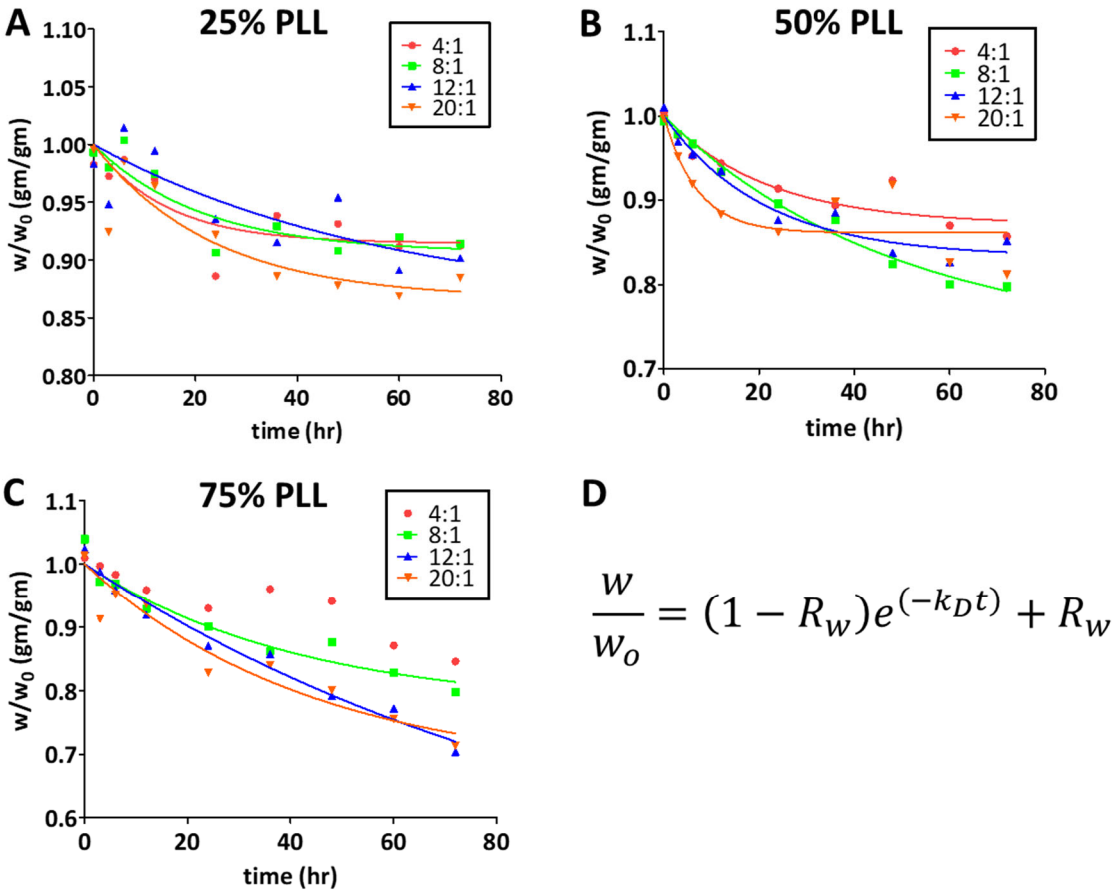

Figure 5. Degradation rates of PEG-PAA-PLL library using A) 25 % PLL B) 50% PLL C) 75% PLL and different ratio of free amines to succinimides. D) The equation modeling the degradation rate, where w is the dry weight of the hydrogel, w_o is the initial dry weight of the hydrogel, k_D is the degradation rate of the gel in trypsin and R_w is the residual weight fraction of the gel, predicting the amount of gel remaining after the PLL in the gel is degraded.

Rheological characterization of two degraded gels (4:1 and 8:1 with 75% PLL) was performed to quantify structural changes from the initial samples. The storage moduli of the degraded gels were observed to decrease by a factor of 20 and 50, respectively, compared to the initial gels (Figure S11). In both cases, the rheological response was indicative of a soft gel; however, the 4:1 gel exhibited transitional behavior at high frequencies, demonstrating the significantly decreased elastically active crosslink density caused by degradation.

k_Dx100(hr^{-1}) R_w (gm/gm)	R^2	4:1		8:1		12:1		20:1	
75% PLL		N/A		2.39 0.77	0.93	0.97 0.44	0.98	2.28 0.67	0.91
50% PLL		4.60 0.87	0.88	2.04 0.73	0.99	4.74 0.83	0.96	14.28 0.86	0.70
25% PLL		6.98 0.91	0.66	4.70 0.91	0.83	1.67 0.86	0.61	4.28 0.87	0.76

Table 1. Degradation rate constants (k_D), residual weight fraction(R_w) and the R^2 values determining the goodness of the fit. (For the samples with 75% PLL and 4:1 ratio the fit was ambiguous, so no model was fit)

Cell survival and capillary-like network formation

Cell survival on the PEG-PAA-PLL library of hydrogels was determined by seeding RECs on top of the hydrogel surface. From the live dead staining, the gels with a lower number of free amines (i.e., the 4:1and 8:1 ratios) showed a relatively higher survival than the other gels in all the three PAA-PLL mixtures (Figure 6A, B). However, after 4 days, most of the cells showed no survival except the 4:1 and 8:1 ratios in the 75% PLL gels and very little survival in the 4:1 ratio of the 50% PLL gel (Figure S12). The cell death is inversely correlated with the primary amine content in the hydrogel, i.e., gels containing a lower amount of amines showed a higher survival (Figure S13A). The 8:1 ratio 75% PLL gel condition, which showed a high initial 4-day survival, also exhibited spreading, migration, and capillary-like network formation at day 4 (Figure 7).

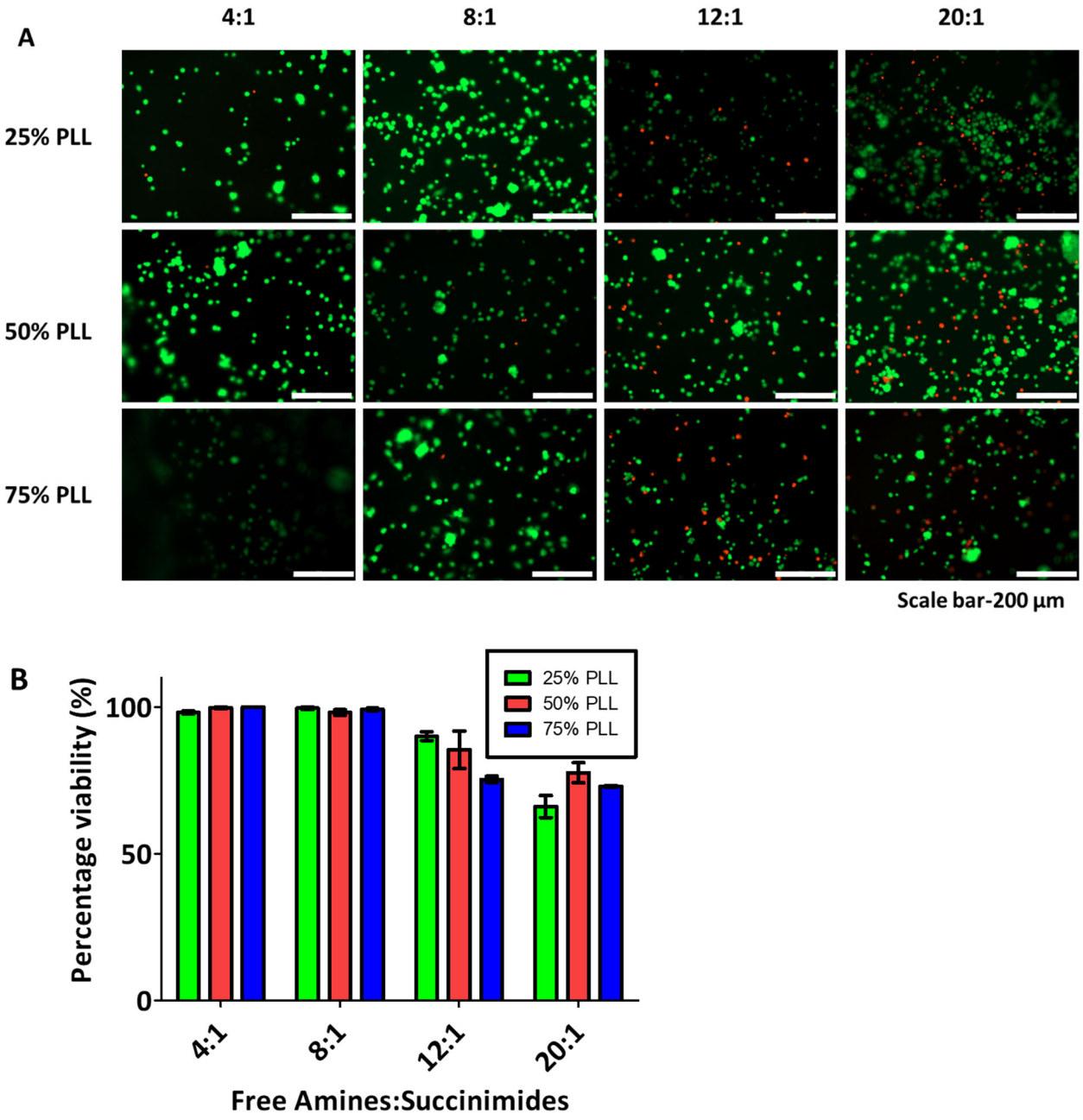

Figure 6. A) Live/ dead scans of rat endothelial cells seeded on the PEG-PAA-PLL hydrogel library (Scale bar is 200 µm) B) Survival of the RECs on the PEG-PAA-PLL hydrogel library

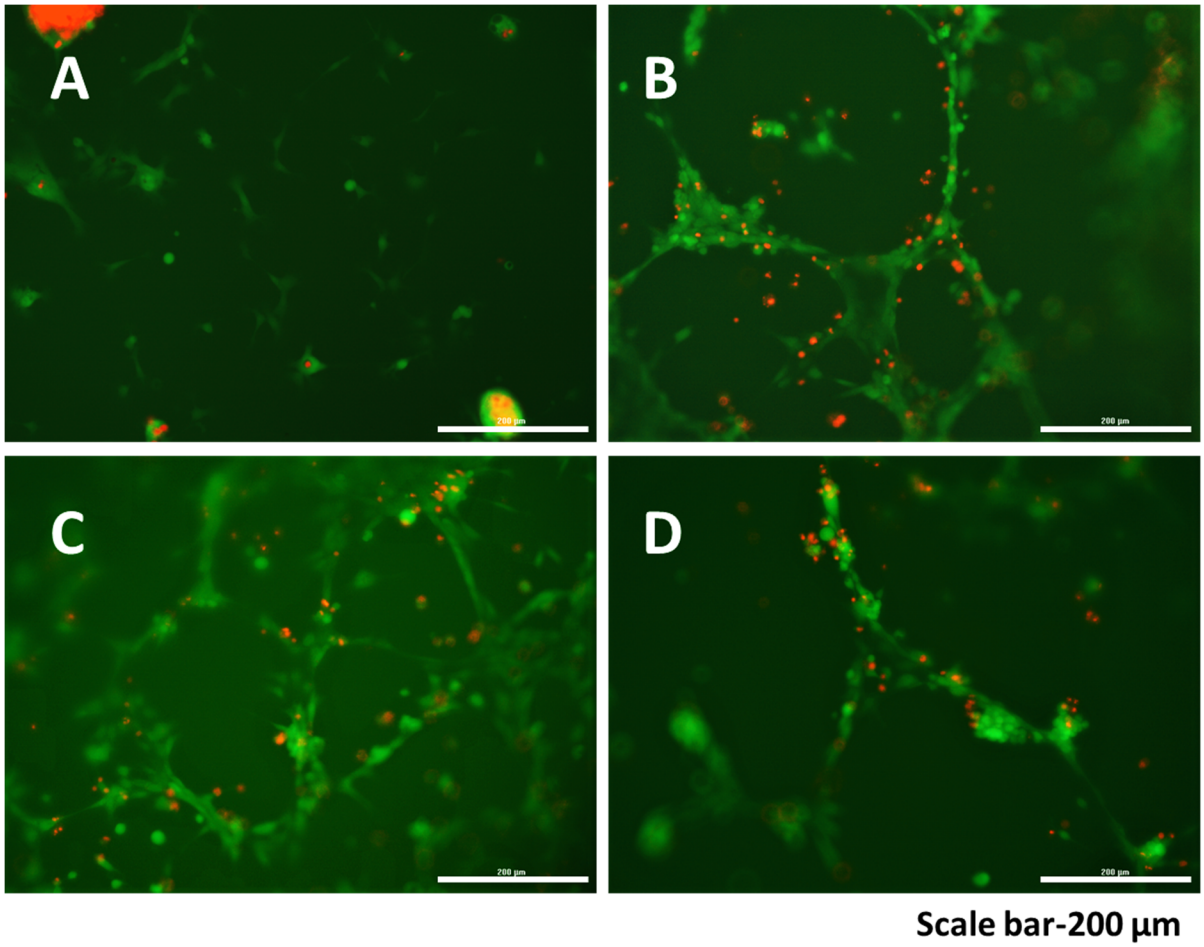

Figure 7. Live/dead scans of the rat endothelial cells A) media control B, C, D, showing cords forming 4 days after seeding on the PEG-PAA-PLL (75% PLL, 8:1 ratio) hydrogel, (Scale bar is 200 µm)

DISCUSSION

The PEG-PAA hydrogel and the semi-degradable PEG-PAA-PLL hydrogel libraries use the succinimidyl-free amine chemistry to form the crosslinked hydrogel network. Since the kinetics of this reaction can range from a few seconds to minutes[18], both these systems can be used to encapsulate cells quickly without the need for external crosslinking agents like temperature or ultraviolet light. In situ rheology of gel formation (Figure S9, for the 4:1 ratio, 25% PLL hydrogel) shows that gelation occurs in tens of minutes at room temperature and can be hastened at physiological conditions. It was observed that storage modulus goes through a maximum with crosslinker content in the PEG-PAA library, demonstrating the limited ability for more crosslinker to produce elastically active chains. The effective molecular weight between crosslinks derived from the elastic modulus is high for all of this gels (Figure S4). This is not surprising based on what we have seen previously with gels synthesized with PEG and PLL [16]. In those gels we saw a structure of walls of gel with micropores around macropores. This heterogenous structure is reflected in the SEM micrographs, particularly Fig. 2C (2:1 ratio) in

which there is a macropore in the center of the image and several micropores. Similar structures are also seen in Figure S5. This large, open porous structure is advantageous for hydrogels for cell models, because these open structures provide space for cells to organize and migrate through the material. The trends observed in the storage modulus of the PEG-PAA system and the PEG-PAA-PLL systems are similar to our previously observed PEG-PLL based hydrogel systems[18]. The reproducibility of the rheological experiments shows that at modest strain amplitudes and axial forces, quantification of the mechanical characteristics of the hydrogels is possible with as-formed gels. These strain amplitudes and axial forces are consistent with biological work[39, 40].

Many hydrogels, either synthetic or derived from native polymers, are degradable. However, loss in the mechanical strength and rigidity of the hydrogel can result in tissue contraction and poor outcomes [41, 42]. Non-degradable hydrogels can maintain mechanically robust structures to facilitate cellular organization into tissues. Non-degradable and partially degradable hydrogels can be used in a setting where long-term cultures are desired for tissue models and regenerative approaches [43-48].

Modifying the PEG-PAA hydrogel system using PLL helped create a new gel system without adding more crosslinkers to help PLL incorporate into the network. Previously many gel systems with tunable degradation rates have been developed[6, 49]. However, the partially degradable nature of the PEG-PAA-PLL hydrogel gives an option for hydrogels that maintain structural rigidity and allow cells to modify the hydrogel with their native proteins. Also, given the ease of synthesis and the kinetics of gel formation[18], both the non-degradable and semi degradable gel systems are suitable for 3D bioprinting and in vitro modeling applications[19, 50]. Previously, we developed a novel bioprinting process based on the traditional lithographic process of screen printing[19], and we have used the PEG-PLL based gels as the bioink in that process[18]. The similar fabrication process and the gelation time (Figure S8) of the current hydrogel systems make them a potential candidate to be easily incorporated in the screen printing process. The PEG-PLL hydrogel shows complete degradation in trypsin within 3 hours. Trypsin cleaves the peptide bond between the individual lysine units in the linear PLL backbone and not the carbamate linkage that leads to the side chains and crosslinks [20, 36]. PAA and PEG are enzymatically and hydrolytically stable, and the PEG-PAA hydrogels do not degrade. This is attractive for long-term cultures. No clear trend was observed from the degradation study in the degradation rates. This may be because the peptide bonds linking individual lysines in the PLL are degraded, but the carbamate bond is not, leaving large fractions of crosslinked chains attached to the network, showing little weight change. Still, there was an order of magnitude change in the G' values. (Figure 5 and Figure S11). The decrease is G' upon degradation suggests that significant bond breakage is occurring; however, the gel response indicates that a percolating network persists. The fact that gels with different starting moduli degrade to the same value suggests a similar gel microstructure remains. A more complete picture of degradation kinetics would likely require rheological studies to characterize the evolving microstructure.

Polycations like PAA are toxic at high concentrations. This toxicity is associated with the cellular membrane disrupting characteristic of high charge densities associated with these cations [51-53]. In lower concentrations or with the absorption of molecules including proteins, polycations are biocompatible materials[24, 54]. Chemical crosslinking can also be toxic to cells, but the SG approach has been used extensively and show low toxicity[55-57]. In this work, we created a library of gels and looked at cell survival. The gels that showed maximum long-term survival, adhesion,

migration, and capillary-like network formation (4:1 and 8:1-75% PLL gels) have a low concentration of PAA in the hydrogel and the lowest number of free amines in the system (Figure S13). The formation of cords suggests that the mechanics and structure of this gel permit endothelial migration and organization consistent with aspects of angiogenesis and vasculogenesis seen in other hydrogels[58, 59]. Promoting microvessels is critical for engineering tissues. However, further work is required to determine if other aspects of angiogenesis are present, including lumens capillary-like networks.

In this work, we focused on the as-made gels without adding proteins or other modifying agents. The presence of the cationic polymers is designed to protein adhesion and provide a foundation for building ECM mimics [23, 27, 60, 61]. As a proof of principle experiment, absorbed laminin in the gel (Figure S7), but these gels can form the basis for more complete models of ECM.

CONCLUSIONS

The PEG-PAA and the PEG-PAA-PLL-based systems provide two unique synthetic hydrogel systems with mechanical properties that can be tuned to be incorporated in long term 3D-cultures. Given the facile nature of the precursor synthesis and hydrogel fabrication, these systems have potential in bioprinting and other process 3D bioprinting applications. Since both the gels systems described here have similar gelation time, kinetics and biocompatibility as the previously developed PLL gels, they can be used in the screen printing process to create in vitro models[18]. We have shown that the semi degradable system supports aspects of angiogenesis and vasculogenesis in vitro, demonstrating its potential as a scaffolding material for other tissue models. Finally, this gel system provides novel semi-degradable biomaterials that can be tuned with regard to degradation, mechanical properties, and chemical cues.

EXPERIMENTAL SECTION

MATERIALS

Poly (allylamine hydrochloride) (120-200kDa) was purchased from Alfa Aeasar, USA. 4arm PEG-Succinimidyl Glutarate(10kDa) was purchased from Jenkem, USA. Acetone, diethyl ether and other solvents, media components (MEM alpha, DMEM, DMEM/F12(Ham)), Fetal Bovine Serum(FBS), HEPES, B27 supplement, N2 supplement, Human epidermal growth gactor (EGF) recombinant protein, Penicillin-Streptomycin, sodium pyruvate, live dead stain, and dialysis tubing were purchased from ThermoFischer Scientific, USA. Linear PEG(4.6kDa), 1,4-Dioxane, poly-L-Lysine (PLL) (70-150kDa), N,N disuccinimidyl carbonate, 4 dimethyl amino pyridine, were purchased from Sigma Aldrich. Caco-2 cells were obtained from ATCC, USA.

METHODS

PEG-SG synthesis

1mmol of PEG solution in dry dioxanes solution is made to a concentration 0.2 gm/ml. Two 12mmol excess solution of N,N Disuccinimidyl carbonate and 4-dimethyl amino pyridine of 0.05gm/ml concentration in acetone are prepared. The three solutions are mixed together and stirred at room temperature for six hours and then the final product is precipitated using diethyl ether. The precipitate is dissolved in deionized water and dialyzed for one hour at room temperature using MWCO-1kDa tubing. The dialyzed product, PEG-SG solution is then flash frozen in liquid nitrogen and lyophilized.

Hydrogel synthesis

10% w/vol solutions of PEG-SG, PLL and PAA in either culture media or 1XPBS were made. The precursor solutions were made in PBS for the rheology, SEM, degradation study and OPA assay. The precursor solutions were made in culture media for cell based experiments. For the cell based experiments, where the PAA precursor solutions were neutralized using sterile NaOH solution. For the hydrogel supplemented with laminin, 1% laminin is added to the PAA precursor solution and incubated at 37°C for an hour before mixing the precursor solutions.

PEG-PAA hydrogels are fabricated by mixing the precursor solutions in the requisite amount based on the ratio of free amines to succinimides. The PAA and PLL solutions are mixed first to make a uniform solution and then mixed with the PEG precursor solution in the required amount to fabricate the PEG-PAA-PLL hydrogel. After mixing the hydrogels all the hydrogels are left to completely set at 37°C for 20 mins. For the cell based experiments the hydrogels are washed with culture media (2x, 5minutes) before cell seeding.

Rheometry

Rheological characterization was performed using 20 mm diameter parallel plates on a DHR-3 rheometer with Peltier heating (TA Instruments, New Castle, DE). Cylindrical hydrogels of approximately 20 mm diameter and 1.5 mm height were fabricated using the above method. Hydrogels were loaded onto the rheometer, which was pre-heated to 37°C, and allowed to equilibrate at that temperature. A nominal axial force of 1 N was applied, such that the gel filled the gap between the plates completely. This force was determined experimentally to produce repeatable results without damaging the gel structure. Frequency sweeps were performed first at nominal, low strain amplitudes (typically $\gamma \approx 0.1\%$), in the range 10^{-1} rad/s $\leq \omega \leq 2 \times 10^{2}$ rad/s.

Strain sweeps were performed to confirm that the chosen amplitude was within the apparent linear viscoelastic regime, which was the case for all reported experiments. In some cases, subsequent frequency sweeps were also performed. Degraded gels were measured using the same protocol, except that samples were trimmed to fill the parallel plate geometry and no axial force was applied because the gels could not sustain force.

In situ gelation experiments were performed to validate measurements of pre-formed gels (i.e., in the absence of potential slip). The requisite solutions of PAA+PLL and PEG were prepared separately, pipetted onto the temperature-controlled rheometer, and gently homogenized before starting the experiment. The experimental protocol consisted of a time sweep, wherein the gel undergoes oscillatory shear at 1 rad/s and 0.1% strain. During this time, a temperature program was applied such that the sample begins at 10°C, ramping to 25°C (2°C/min) where it remains constant for 1 hr, followed by a ramp to 37°C where it remains constant for 0.5 hr. These conditions were chosen to slow gelation during sample loading and mixing and to match pre-formed gel formation conditions. After formation, the typical protocol used above was applied.

Scanning Electron Microscopy

The fabricated hydrogels were swollen in excess of water overnight at room temperature, the excess water was removed, and the gels were frozen at -20ºC overnight and then flash frozen using liquid nitrogen, and lyophilized for two days. 20nm layer of gold palladium was coated onto the dried hydrogel using a vacuum sputter coater (Denton Desk II) and the sample was imaged using a Nova NanoSEM 450(FEI).

Nuclear Magnetic Resonance

NMR spectrum of the synthesized PEG-SG was measure using JEOL 400Mhz NMR system, with an ~10mg/ml analyte solution in deuterated water.

Degradation and Swelling study

The precursor solutions were mixed according to the ratio of free amines to succinimides to total volume of 500ul of gel. The weight of the hydrogel is noted after complete gelation. 700 ul of 0.05% Trypsin-EDTA was added to the hydrogel and incubated at 37ºC. Excess trypsin was removed at each time point and the hydrogel is flash frozen and lyophilized. Then the dry weight of the hydrogel was measured. The degradation kinetics are modeled using the one phase decay models using GraphPad Prism.

Cell culture

Rat endothelial cells were cultured in DMEM High Glucose supplemented with 10% FBS, 1% HEPES, and 1% Sodium pyruvate. Caco-2 cells were cultured in MEM alpha supplemented with 20% FBS. For the cord formation assay we used conditioned neural progenitor cell (NPC) media mixed at 1:1 ratio with the REC media, for all the conditions including the controls. NPCs were cultured in media is composed of DMEM/F12(Ham) supplemented with B27, N2, EGF (20ng/ml), and Penicillin-Streptomycin. The NPC media is collected after week of culture, sterile filtered and frozen in aliquots. This is used as the conditioned NPC media in the cord formation assay.

Live/Dead assay

A mixture containing 4 µm of calcien-AM and 8µm of ethidium homodimer was used as the live/dead stain. The stain was added to the cells and imaged after 30 minutes of incubation at 37ºC and 5% CO_2. The cells are then imaged using Cytation 5 (Biotek, USA).

O-phthalaldehyde (OPA) assay

OPA assay was performed as described by Grotzky et.al. [62] using premade hydrogels against a standard curve of Poly-L-Lysine. All the gels and the standards were prepared in 1X PBS.

REFERENCES

1. S. R. Caliari and J. A. Burdick, *Nature methods*, 2016, **13**, 405-414.
2. J. Li and D. J. Mooney, *Nature Reviews Materials*, 2016, **1**, 16071.
3. Z. Zhao, C. Vizetto-Duarte, Z. K. Moay, M. I. Setyawati, M. Rakshit, M. H. Kathawala and K. W. Ng, *Frontiers in Bioengineering and Biotechnology*, 2020, **8**.
4. L. J. Bray, M. Binner, U. Freudenberg and C. Werner, *Methods in molecular biology (Clifton, N.J.)*, 2017, **1612**, 39-63.
5. R. Cruz-Acuña, M. Quirós, A. E. Farkas, P. H. Dedhia, S. Huang, D. Siuda, V. García-Hernández, A. J. Miller, J. R. Spence, A. Nusrat and A. J. García, *Nature Cell Biology*, 2017, **19**, 1326-1335.
6. S. P. Zustiak and J. B. Leach, *Biomacromolecules*, 2010, **11**, 1348-1357.
7. E. A. Aisenbrey and W. L. Murphy, *Nature reviews. Materials*, 2020, **5**, 539-551.
8. M. C. Catoira, L. Fusaro, D. Di Francesco, M. Ramella and F. Boccafoschi, *J Mater Sci Mater Med*, 2019, **30**, 115.
9. C. S. Hughes, L. M. Postovit and G. A. Lajoie, *Proteomics*, 2010, **10**, 1886-1890.
10. N. C. Talbot and T. J. Caperna, *Cytotechnology*, 2015, **67**, 873-883.
11. E. Davison-Kotler, W. S. Marshall and E. García-Gareta, *Bioengineering (Basel)*, 2019, **6**, 56.
12. S. J. Bryant, R. J. Bender, K. L. Durand and K. S. Anseth, *Biotechnology and bioengineering*, 2004, **86**, 747-755.
13. J. Zhu, *Biomaterials*, 2010, **31**, 4639-4656.
14. C.-C. Lin and K. S. Anseth, *Pharmaceutical Research*, 2009, **26**, 631-643.
15. G. M. Fernandes-Cunha, K. M. Chen, F. Chen, P. Le, J. H. Han, L. A. Mahajan, H. J. Lee, K. S. Na and D. Myung, *Scientific reports*, 2020, **10**, 16671.
16. S. Royce Hynes, L. M. McGregor, M. Ford Rauch and E. B. Lavik, *Journal of biomaterials science. Polymer edition*, 2007, **18**, 1017-1030.
17. S. R. Hynes, M. F. Rauch, J. P. Bertram and E. B. Lavik, *J Biomed Mater Res A*, 2009, **89**, 499-509.
18. N. Pandala, M. A. LaScola, Y. Tang, M. Bieberich, L. T. J. Korley and E. Lavik, *ACS Biomater Sci Eng*, 2021, DOI: 10.1021/acsbiomaterials.1c00902.
19. N. Pandala, S. Haywood, M. A. LaScola, A. Day, J. Leckron and E. Lavik, *ACS Applied Bio Materials*, 2020, **3**, 8113-8120.
20. G. T. Hermanson, in *Bioconjugate Techniques (Third Edition)*, ed. G. T. Hermanson, Academic Press, Boston, 2013, DOI: https://doi.org/10.1016/B978-0-12-382239-0.00003-0, pp. 229-258.
21. M. F. Rauch, M. Michaud, H. Xu, J. A. Madri and E. B. Lavik, *Journal of biomaterials science. Polymer edition*, 2008, **19**, 1469-1485.
22. M. S. Sarwar, Q. Huang, A. Ghaffar, M. A. Abid, M. S. Zafar, Z. Khurshid and M. Latif, *Pharmaceutics*, 2020, **12**.
23. O. Boussif, T. Delair, C. Brua, L. Veron, A. Pavirani and H. V. J. Kolbe, *Bioconjugate Chemistry*, 1999, **10**, 877-883.
24. M. Wytrwal and C. Pichon, *Methods in molecular biology (Clifton, N.J.)*, 2016, **1445**, 159-174.
25. J. M. Giussi, M. Martínez Moro, A. Iborra, M. L. Cortez, D. Di Silvio, I. Llarena Conde, G. S. Longo, O. Azzaroni and S. Moya, *Soft Matter*, 2020, **16**, 881-890.
26. D. D. Iarikov, M. Kargar, A. Sahari, L. Russel, K. T. Gause, B. Behkam and W. A. Ducker, *Biomacromolecules*, 2014, **15**, 169-176.
27. S. Duggan, H. Hughes, E. Owens, E. Duggan, W. Cummins and O. D. O, *International journal of pharmaceutics*, 2016, **499**, 368-375.
28. L. Alekseenko, M. Shilina, I. Kozhukharova, O. Lyublinskaya, I. Fridlyanskaya, N. Nikolsky and T. Grinchuk, *Cells*, 2020, **9**.

29. S. Kagaya, Y. Saeki, D. Morishima, T. Kajiwara, W. Kamichatani, H. Yanai, T. Katoh, M. Saito, M. Gemmei-Ide and Y. Inoue, *Analytical sciences : the international journal of the Japan Society for Analytical Chemistry*, 2020, **36**, 583-588.
30. S. Sabouri-Rad, R. K. Oskuee, A. Mahmoodi, L. Gholami and B. Malaekeh-Nikouei, *BioImpacts : BI*, 2017, **7**, 139-145.
31. K. K. Kang, H. S. Oh, D. Y. Kim, G. Shim and C. S. Lee, *Journal of colloid and interface science*, 2017, **507**, 145-153.
32. V. Adibnia and R. J. Hill, *Journal of Rheology*, 2016, **60**, 541-548.
33. F. Abd-El Salam, M. H. Abd-El Salam, M. T. Mostafa, M. R. Nagy and M. I. Mohamed, *Journal of Applied Polymer Science*, 2003, **90**, 1539-1544.
34. D. Calvet, J. Y. Wong and S. Giasson, *Macromolecules*, 2004, **37**, 7762-7771.
35. S. Seiffert, *Polymer Chemistry*, 2017, **8**, 4472-4487.
36. Z. Kadlecova, L. Baldi, D. Hacker, F. M. Wurm and H.-A. Klok, *Biomacromolecules*, 2012, **13**, 3127-3137.
37. W. M. Kulicke, Y. A. Aggour, H. Nottelmann and M. Z. Elsabee, *Starch - Stärke*, 1989, **41**, 140-146.
38. N. A. Peppas and E. W. Merrill, *Journal of Applied Polymer Science*, 1977, **21**, 1763-1770.
39. K. J. Jeong and A. Panitch, *Biomacromolecules*, 2009, **10**, 1090-1099.
40. J. M. Zuidema, C. J. Rivet, R. J. Gilbert and F. A. Morrison, *J Biomed Mater Res B Appl Biomater*, 2014, **102**, 1063-1073.
41. H. Tan and K. G. Marra, *Materials (Basel)*, 2010, **3**, 1746-1767.
42. P. M. Kharkar, K. L. Kiick and A. M. Kloxin, *Chemical Society Reviews*, 2013, **42**, 7335-7372.
43. S. Dobner, D. Bezuidenhout, P. Govender, P. Zilla and N. Davies, *Journal of cardiac failure*, 2009, **15**, 629-636.
44. S. A. Maher, S. B. Doty, P. A. Torzilli, S. Thornton, A. M. Lowman, J. D. Thomas, R. Warren, T. M. Wright and E. Myers, *Journal of biomedical materials research. Part A*, 2007, **83**, 145-155.
45. D. A. Bichara, X. Zhao, N. S. Hwang, H. Bodugoz-Senturk, M. J. Yaremchuk, M. A. Randolph and O. K. Muratoglu, *The Journal of surgical research*, 2010, **163**, 331-336.
46. W. Swieszkowski, D. N. Ku, H. E. Bersee and K. J. Kurzydlowski, *Biomaterials*, 2006, **27**, 1534-1541.
47. M. Kobayashi, J. Toguchida and M. Oka, *Journal of biomedical materials research*, 2001, **58**, 344-351.
48. G. H. Underhill, A. A. Chen, D. R. Albrecht and S. N. Bhatia, *Biomaterials*, 2007, **28**, 256-270.
49. F.-Y. Lin and C.-C. Lin, *ACS Macro Letters*, 2021, **10**, 341-345.
50. E. Mancha Sánchez, J. C. Gómez-Blanco, E. López Nieto, J. G. Casado, A. Macías-García, M. A. Díaz Díez, J. P. Carrasco-Amador, D. Torrejón Martín, F. M. Sánchez-Margallo and J. B. Pagador, *Frontiers in Bioengineering and Biotechnology*, 2020, **8**.
51. W. Kopec, A. Żak, D. Jamróz, R. Nakahata, S.-I. Yusa, V. Gapsys and M. Kepczynski, *Langmuir*, 2020, **36**, 12435-12450.
52. D. Fischer, Y. Li, B. Ahlemeyer, J. Krieglstein and T. Kissel, *Biomaterials*, 2003, **24**, 1121-1131.
53. S. M. Moghimi, P. Symonds, J. C. Murray, A. C. Hunter, G. Debska and A. Szewczyk, *Molecular therapy : the journal of the American Society of Gene Therapy*, 2005, **11**, 990-995.
54. M. Wytrwal, P. Koczurkiewicz, K. Wójcik, M. Michalik, B. Kozik, M. Zylewski, M. Nowakowska and M. Kepczynski, *Journal of biomedical materials research. Part A*, 2014, **102**, 721-731.
55. C. Lotz, F. F. Schmid, E. Oechsle, M. G. Monaghan, H. Walles and F. Groeber-Becker, *ACS applied materials & interfaces*, 2017, **9**, 20417-20425.
56. H. Chen, F. Fei, X. Li, Z. Nie, D. Zhou, L. Liu, J. Zhang, H. Zhang, Z. Fei and T. Xu, *Bioactive materials*, 2021, **6**, 3580-3595.

57. Z. Wu, S. H. Korntner, J. Olijve, A. M. Mullen and D. I. Zeugolis, *Biomolecules*, 2021, **11**.
58. I. Arnaoutova, J. George, H. K. Kleinman and G. Benton, *Angiogenesis*, 2009, **12**, 267-274.
59. G. Benton, I. Arnaoutova, J. George, H. K. Kleinman and J. Koblinski, *Adv Drug Deliv Rev*, 2014, **79-80**, 3-18.
60. W. M. Huang, S. J. Gibson, P. Facer, J. Gu and J. M. Polak, *Histochemistry*, 1983, **77**, 275-279.
61. M. S. Liberio, M. C. Sadowski, C. Soekmadji, R. A. Davis and C. C. Nelson, *PloS one*, 2014, **9**, e112122-e112122.
62. A. Grotzky, Y. Manaka, S. Fornera, M. Willeke and P. Walde, *Analytical Methods*, 2010, **2**, 1448-1455.